Volatility Project

Student Name: Nguyen Ngoc Truong
Student ID: [20235264]

Student Name: Khalil Hassan
Student ID: [20234229]

Student Name: Francesco Cojutti
Student ID: [ERASMUS]

August 1, 2024

Contents

List of Figures

List of Tables

1. Estimation of the parameter H

1.1 Enhanced Heston Model Trajectory

Within the framework of an enhanced Heston model characterized by parameters $n = 20$, initial variance $V_0 = 0.05$, mean reversion speed $\lambda = 0.3$, long-term variance $\theta = 0.05$, volatility of variance $\nu = 0.1$, $\alpha = H + 0.5 = 0.6$, and a leverage factor of $r_{20} = 2.5$, we illustrate the trajectory of the variance process V_{tk} across the span $[0, 1]$. This is achieved through a uniform segmentation defined as $t_0 = 0, t_1 = \Delta t, \ldots, t_m = m\Delta t$, where $m = 10^5$.

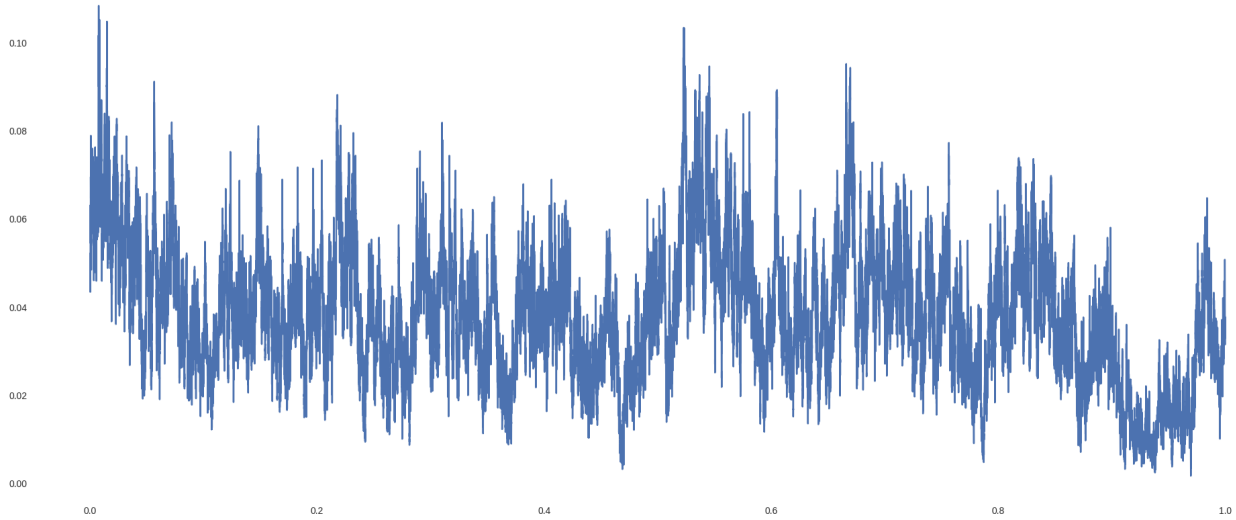

Figure 1.1: Trajectory of Variance in an Enhanced Heston Framework

1.2 Estimation of Hurst Parameter H

To deduce the Hurst parameter H utilizing the approach outlined in the first lecture, we start with the practical computation of moments:

$$m(q, \Delta) = \frac{1}{m_\Delta} \sum_{i=1}^{m_\Delta} |Vt_{k+\Delta} - V_t|^q$$

Subsequently, we determine the optimal ζ_q for each q to express $\log(m(q, \Delta))$ as a linear function of $\log(\Delta)$:

$$\log(m(q, \Delta)) = \zeta_q \cdot \log(\Delta) + C_q$$

Thus, the linear regression slope of ζ_q against q reveals the Hurst parameter H.

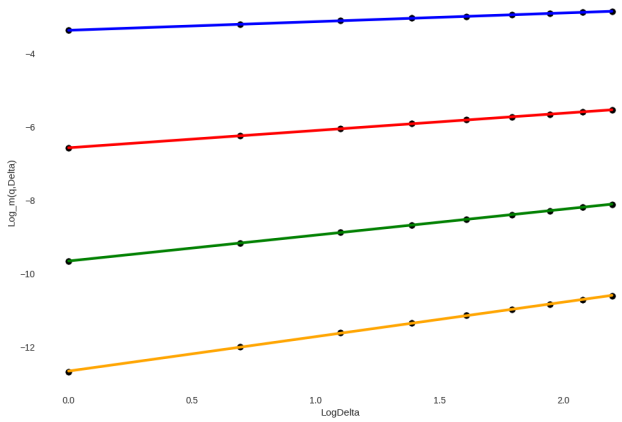

Figure 1.2: Estimation of H via Linear Regression

The estimated value of H is 0.467. This value is close to 0.5 (The Hurst parameter for a standard Brownian motion). Since volatility is a function of standard Brownian motion. Hence, the H value we estimated is close to our expectations.

1.3 Refinement of H Estimation

The plot of H's estimations as a function of l's values (control the sampling frequency) is displayed below:

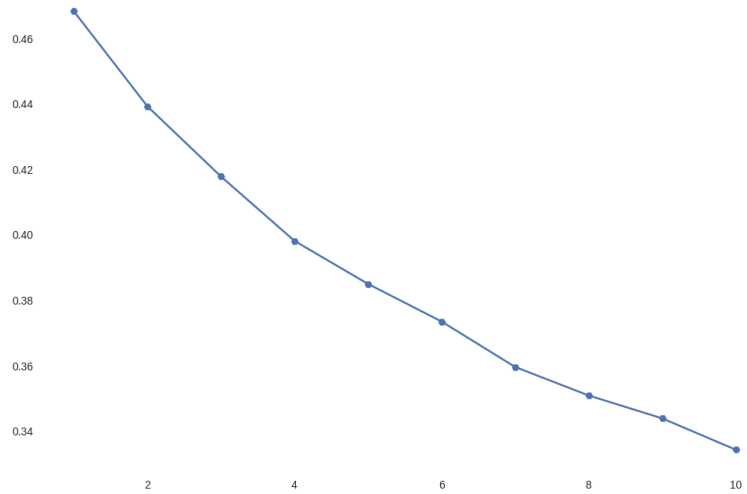

Figure 1.3: Variation of $H(l)$ Relative to Sampling Density

We observe that the more we decrease the sampling frequency of the volatility, the smaller is H, which means that the standard Brownian motion is not the convenient random process to model the volatility.

1.4 Standard Brownian Motion Analysis

Repeating the procedures from path simulation to the estimation of H, this time for a standard Brownian motion W_t.

The simulation of one path of a standard Brownian motion is displayed below:

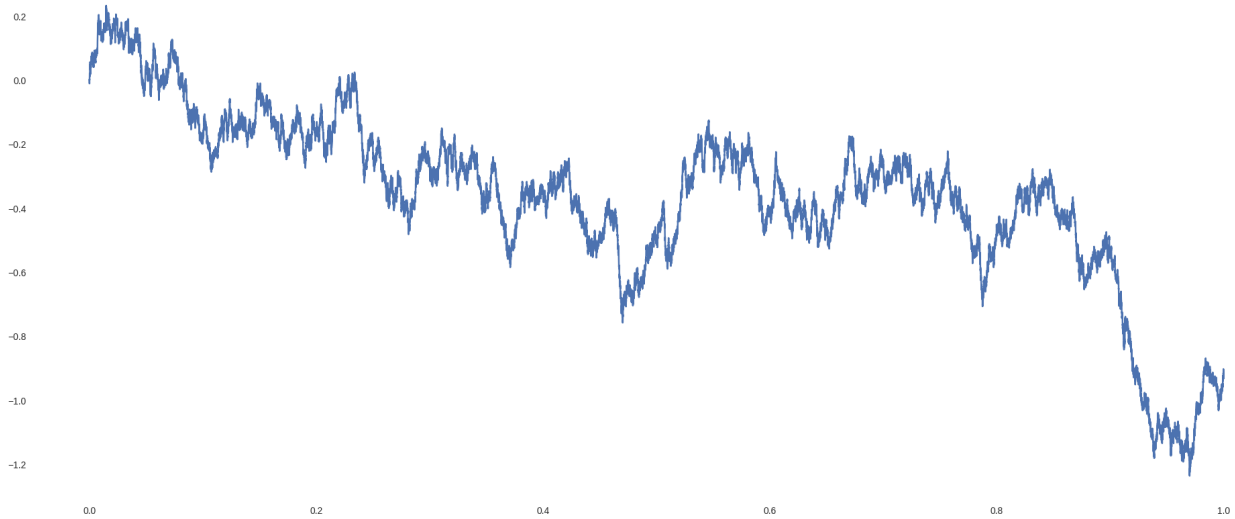

Figure 1.4: Path of Standard Brownian Motion

For this scenario, empirical moments are given by:

$$m(q, \Delta) = \frac{1}{m_\Delta} \sum_{i=1}^{m_\Delta} |W_{t_{k+\Delta t}} - W_{t_k}|^q$$

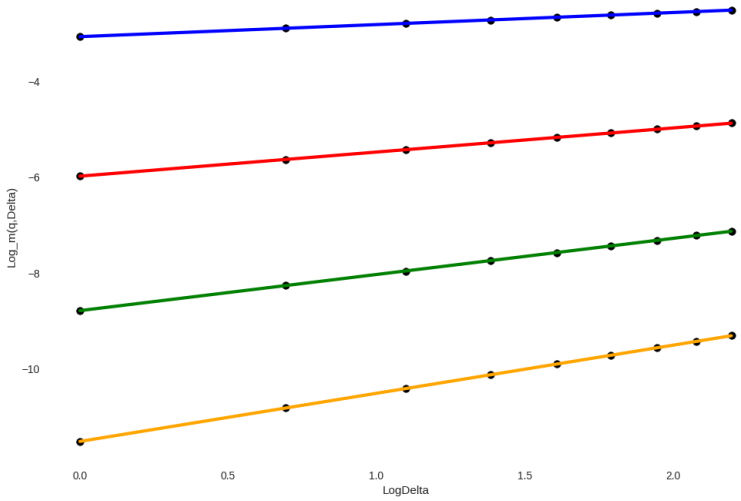

Figure 1.5: Estimation of H via Linear Regression

The estimated value of H is 0.49, which aligns with the theoretical value of the Hurst parameter of a standard Brownian Motion, which is equal to 0.5.

The plot of H's estimations as a function of l's values (control the sampling frequency) is displayed below:

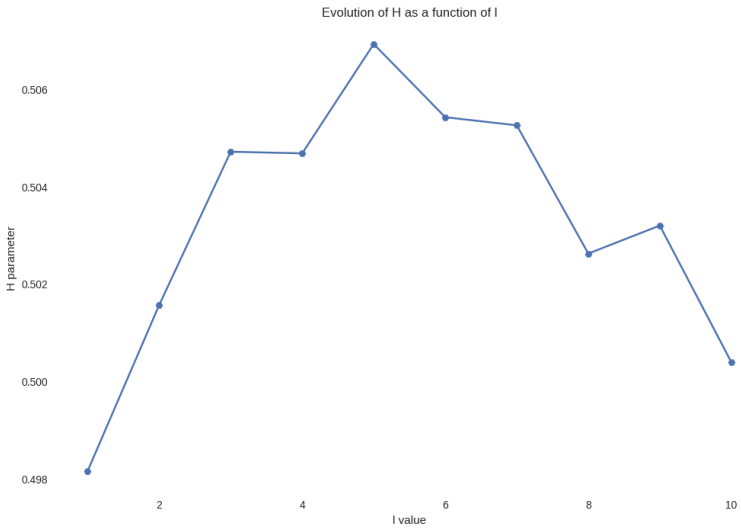

Figure 1.6: Variation of H(l) Relative to the sampling Density

We observe that when we reduce the sampling frequency of the BM Vector, the value of H value is always around 0.5, which implies that the roughness of a standard Brownian Motion is stable even with reducing the sampling frequency and demonstrates again that the value of the Hurst parameter to chose to model a standard Brownian Motion using a fractional Brownian Motion is 0.5.

1.5 Fractional Brownian Motion Analysis

Substituting V with a fractional Brownian motion W^H (H $= 0.1$), the process W^H is characterized by:

$$E[W_t^H W_s^H] = \frac{1}{2}(|t|^{2H} + |s|^{2H} - |t-s|^{2H})$$

Using Cholesky decomposition for simulation over a grid with $m = 10^3$ ($\Delta t = 10^{-3}$), we derive the simulation of one path of a fractional Brownian motion (H=0.1) as follows:

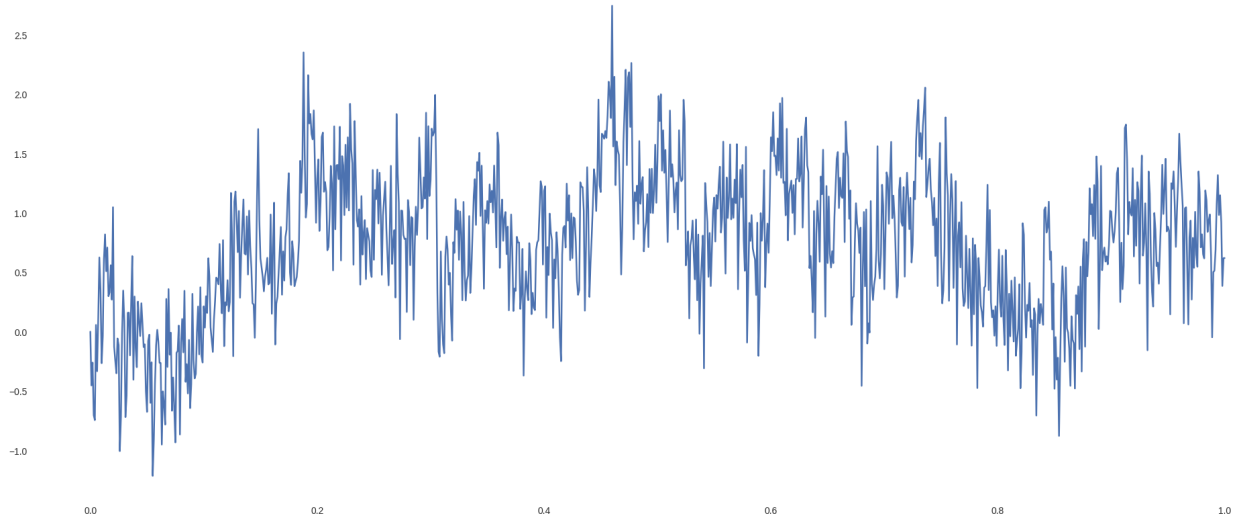

Figure 1.7: Fractional Brownian Motion (H = 0.1) Path

For this scenario, empirical moments are given by:

$$m(q, \Delta) = \frac{1}{m_\Delta} \sum_{i=1}^{m_\Delta} |W^H_{t_{k+\Delta t}} - W^H_{t_k}|^q$$

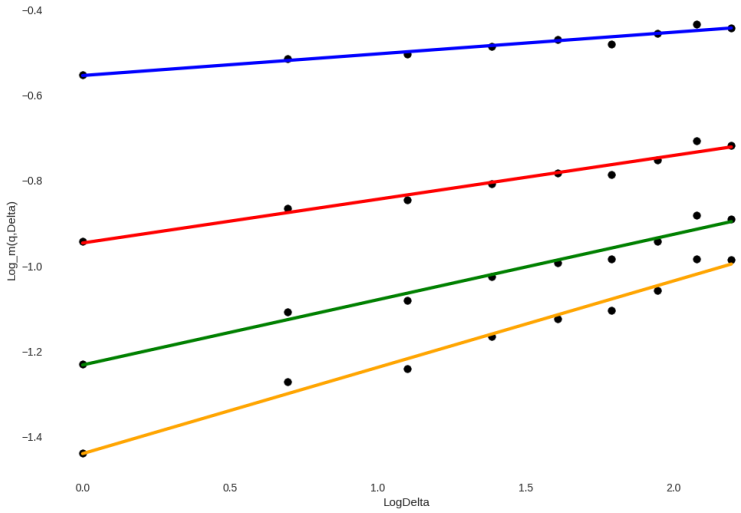

Figure 1.8: Estimation of H via Linear Regression

The estimated H is given by 0.1, which is precisely the one that we used to simulate the Fractional Brownian Motion vector.

The plot of H's estimations as a function of l's values (control the sampling frequency) is displayed below:

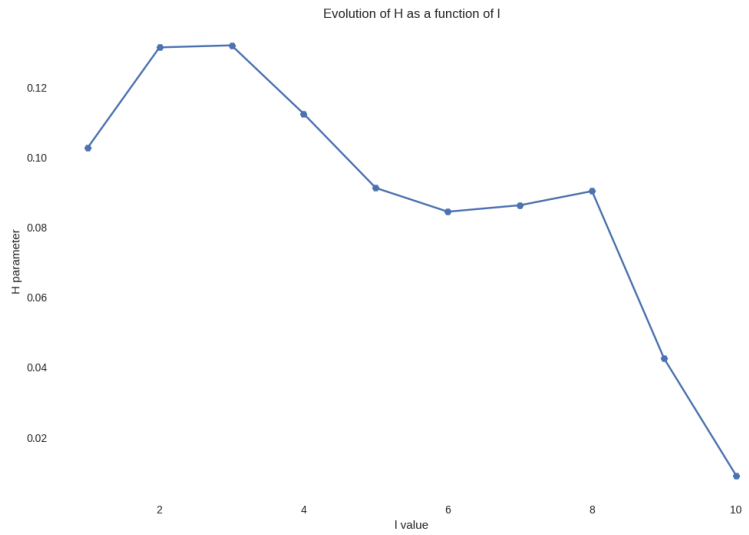

Figure 1.9: Variation of H(l) Relative to the sampling Density

We observe a decreasing trend of H when we decrease the sampling frequency of the W^H vector (contrary to the standard Brownian motion), demonstrating that the vector becomes rougher when we decrease the sampling frequency.

2. Implied volatility in the Lifted Heston model

1. a) Deduce by Itô's formula that M is a local martingale

First, we have the price-variance dynamic from slide 12 of Part III:

$$dS_t = S_t\sqrt{V_t}dB_t \quad \text{(discounted price)} \tag{2.1}$$

$$V_t = g_0(t) + \sum_{i=1}^{n} c_i U_t^i \tag{2.2}$$

$$dU_t^i = (-x_i U_t^i - \lambda V_t)dt + \nu\sqrt{V_t}dW_t \tag{2.3}$$

with $d\langle B, W\rangle_t = \rho dt$

Second, from the slide 14 of Part III:

$$\begin{aligned}(\psi^j)' &= -x_i\psi^j + F\left(u, \sum_{j=1}^{n} c_j\psi^j\right) \\ F(u,v) &= \frac{1}{2}(u^2 - u) + (\rho\nu u - \lambda v)u + \frac{\nu^2}{2}v^2\end{aligned} \tag{2.4}$$

and

$$\phi(t,T) = \int_0^{T-t} F\left(u, \sum_{j=1}^{n} c_j\psi^j(s)\right) g_0(T-s)ds \tag{2.5}$$

From (2.1), using Itô's formula, we have :

$$d\log(S_t) = -\frac{V_t}{2}dt + \sqrt{V_t}dB_t \tag{2.6}$$

and

$$M_t = \exp\left(u\log(S_t) + \phi(t,T) + \sum_{i=1}^{n} c_i\psi^i(T-t)U_t^i\right) \tag{2.7}$$

We have:

$$\begin{aligned}\frac{dM_t}{M_t} = \Bigg[& u\left(-\frac{V_t}{2}\right) + \phi'(t,T) + \sum_{i=1}^{n} c_i \psi^i(T-t)\left(-x_i U_t^i - \lambda V_t\right) \\ & - \sum_{i=1}^{n} c_i (\psi^i)'(T-t) U_t^i + \frac{1}{2}u^2 V_t + \frac{1}{2}\left(\sum_{i=1}^{n} c_i \psi^i(T-t)\right)^2 \nu^2 V_t \\ & + u \sum_{i=1}^{n} c_i \psi^i(T-t)\rho\nu V_t \Bigg] dt + H_t\end{aligned}$$

Using (2.2):

$$\begin{aligned}= \Bigg[& \phi'(t,T) + \frac{1}{2}(u^2-u) g_0(t) - \lambda \left[\sum_{i=1}^{n} c_i \psi^i(T-t)\right] g_0(t) \\ & + \frac{1}{2}\left(\sum_{i=1}^{n} c_i \psi^i(T-t)\right)^2 \nu^2 g_0(t) + \rho\nu u \left(\sum_{i=1}^{n} c_i \psi^i(T-t)\right) g_0(t) \Bigg] dt \\ & + \sum_{i=1}^{n} c_i U_t^i \Bigg[\frac{1}{2}(u^2-u) - x_i \psi^i(T-t) - (\psi^i)'(T-t) \\ & - \lambda \sum_{j=1}^{n} c_j \psi^j(T-t) - \phi'(t,T)\frac{1}{2}\nu^2 \left(\sum_{j=1}^{n} c_j \psi^j(T-t)\right)^2 \\ & + \rho\nu u \left(\sum_{j=1}^{n} c_j \psi^j(T-t)\right) \Bigg] dt + H_t\end{aligned}$$

Using (2.4) and (2.5):

$$\begin{aligned}= & \left[\phi'(t,T) + g_0(t) F\left(u, \sum_{j=1}^{n} c_j \psi^j(T-t)\right)\right] dt \\ & + \sum_{i=1}^{n} c_i U_t^i \Bigg[-(\psi^i)'(T-t) - x_i \psi^i(T-t) \\ & + F\left(u, \sum_{j=1}^{n} c_j \psi^j(T-t)\right) \Bigg] dt + H_t \\ = & \; H_t\end{aligned} \tag{2.8}$$

with H_t being a local martingale component
So we have M_t is a local martingale

b) If M is a true martingale, then:

$$\begin{aligned} Mt &= \mathbb{E}\left[M_T | \mathcal{F}_t\right] \\ &= \mathbb{E}\left[\exp\left(u \log S_T + \phi\left(T,T\right) + \sum_{i=1}^{n} c_i \psi^i(0)\right) | \mathcal{F}_t\right] \\ &= \mathbb{E}\left[\exp(u \log S_T) | \mathcal{F}_t\right] \end{aligned} \tag{2.9}$$

because $\psi^i(0)$ and $\phi\left(T,T\right) = 0$

2. Carr-Madan formula
Define the risk-neutral density $\log S_t$ is $q_T(s)$ and $k = \log K$, so we have the initial call

value C_0 is:

$$C_0 = \int_k^\infty e^{-r_{int}T}(e^s - e^k)q_T(s)\,ds. \tag{2.10}$$

We have by dominated convergence that C_0 tends to S_0 as k tends to $-\infty$, and hence the call pricing function is not square integrable $\left(\int_{-\infty}^{\infty} C_0^2 ds = \infty\right)$. To obtain a square-integrable function, following the idea from Slide 21 Part II, we consider the modified call price c_0 defined by:

$$c_0 = \exp(\alpha_2 k)C_0 \tag{2.11}$$

for $\alpha_2 > 0$. Consider now the Fourier transform of c_0 defined by:

$$\psi_0(u) = \int_{-\infty}^{\infty} e^{iuk}c_0\,dk. \tag{2.12}$$

Using the inverse transform, we have:

$$\begin{aligned} C_0 &= \frac{\exp(-\alpha_2 k)}{2\pi}\int_{-\infty}^{\infty} e^{-iuk}\psi_0(u)\,du \\ &= \frac{\exp(-\alpha_2 k)}{\pi}\int_0^{\infty} \Re\left\{e^{-iuk}\psi_0(u)\right\}\,du. \end{aligned} \tag{2.13}$$

The second equality holds because C_0 is real, and the conjugate complex of $e^{-iuk}\psi_0(u)$ is $e^{iuk}\psi_0(-u)$.

The expression for $\psi_0(u)$ is determined from (2.11) and (2.12) as follows:

$$\begin{aligned} \psi_0(u) &= \int_{-\infty}^{\infty} e^{iuk}\int_k^{\infty} e^{\alpha_2 k}e^{-r_{int}T}(e^s - e^k)q_T(s)\,dsdk \\ &= \int_{-\infty}^{\infty} e^{-r_{int}T}q_T(s)\int_{-\infty}^{s} e^{iuk}e^{\alpha_2 k}(e^s - e^k)dk\,ds \\ &= \int_{-\infty}^{\infty} e^{-r_{int}T}q_T(s)\int_{-\infty}^{s} \left(e^s e^{(\alpha_2+iu)k} - e^{(\alpha_2+iu+1)k}\right)dk\,ds \\ &= \int_{-\infty}^{\infty} e^{-r_{int}T}q_T(s)\left[\frac{e^{(\alpha_2+1+iu)s}}{\alpha_2+1+iu} - \frac{e^{(\alpha_2+1+iu)k}}{\alpha_2+1+iu}\right]_{-\infty}^{s} ds \\ &= \int_{-\infty}^{\infty} e^{-r_{int}T}q_T(s)\left[\frac{e^{(\alpha_2+1+iu)s}}{\alpha_2+iu} - \frac{e^{(\alpha_2+1+iu)s}}{\alpha_2+1+iu}\right] ds \\ &= \frac{e^{-r_{int}T}}{(\alpha_2+iu)(\alpha_2+1+iu)}\int_{-\infty}^{\infty} q_T(s)e^{is*(u-(\alpha_2+1)i)} \\ &= e^{-r_{int}T}\frac{\Phi_T\left(u-(\alpha_2+1)\,i\right)}{(\alpha_2+iu)(\alpha_2+1+iu)} \end{aligned} \tag{2.14}$$

From line 1 to line 2, we use the Fubini theorem to change the order of integration, and from line 6 to line 7, we use the definition of characteristic function.

Now, replace (2.14) into (2.13), and replace k with $\log K$, we have:

$$C_0 = \frac{e^{-r_{\text{int}}T-\alpha_2\log(K)}}{\pi}\int_0^{\infty} \Re\left(\frac{\Phi_T(u-(\alpha_2+1)i)}{(\alpha_2+iu)(\alpha_2+1+iu)}e^{-i\log(K)u}\right)du \tag{2.15}$$

For questions 2.3, 2.4, and 2.5, all the derived functions with detailed steps are shown in

the Jupyter Notebook Exercise 2.ipynb

5. Plot the implied volatility smiles for $n = 5, 10, 20, 50$

   a) $T = 1, L = 100$ with 20 equidistant log strikes between -1.2 and 0.2

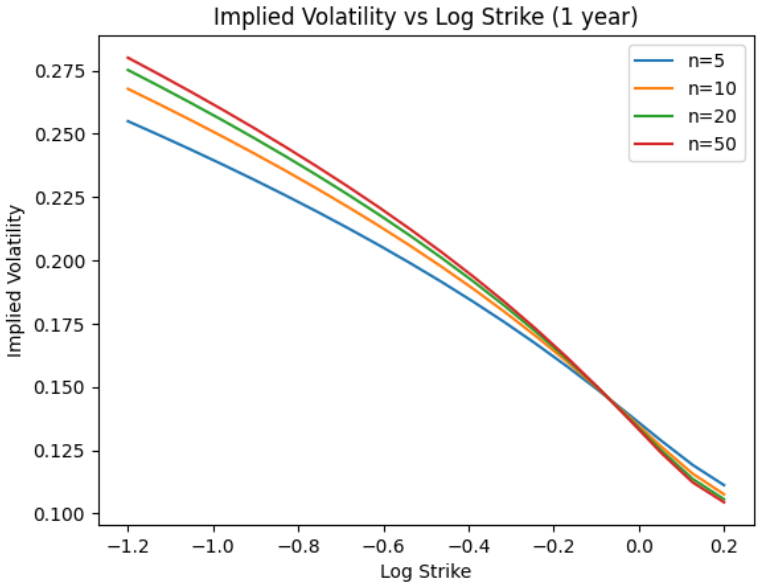

Figure 2.1: Implied Volatility vs Log Strike (1 year)

From the graph, we can see that:

- For all factors, the slope of the implied volatility curve indeed indicates that as options go from ITM to ATM to OTM (as $\log K$ increases), the implied volatility tends to decrease, which is in line with typical market observations where there's less demand (and therefore, lower implied volatility) for far OTM call options compared to closer to ATM options.
- As the number of factors increases, the lines appear to converge, especially between n=20 and n=50, which indicates that adding more factors to the model may only marginally improve the fit to market data.

   b) $T = 1/26, L = 1000$ with 20 equidistant log strikes between -0.15 and 0.05

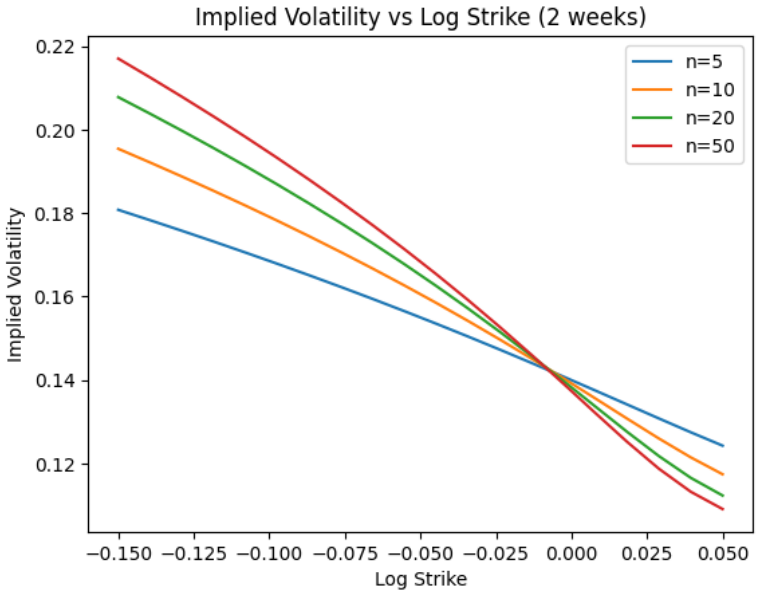

Figure 2.2: Implied Volatility vs Log Strike (2 weeks)

- The implied volatility behavior for ITM, ATM, and OTM are the same compared to previous cases
- The slope of the implied volatility curves for the short-term options is steeper compared to the one-year options, suggesting that the short-term market expectations of volatility are more sensitive to changes in the strike price
- Similar to the one-year case, the curves for different numbers of factors ($n = 5, 10, 20, 50$) seem to converge as the number of factors increases. However, this might be less pronounced over the short maturity, indicating that the market views near-term events as less predictable or more volatile.

3. Implied volatility in the Lifted/Rough Bergomi model

For questions 3.1,3.2, and 3.3, all the derived functions with detailed steps are shown in the Jupyter Notebook Exercise 3.ipynb

1. Based on the given parameter from 3.3, we draw 4 sample trajectories for V_t and S_t

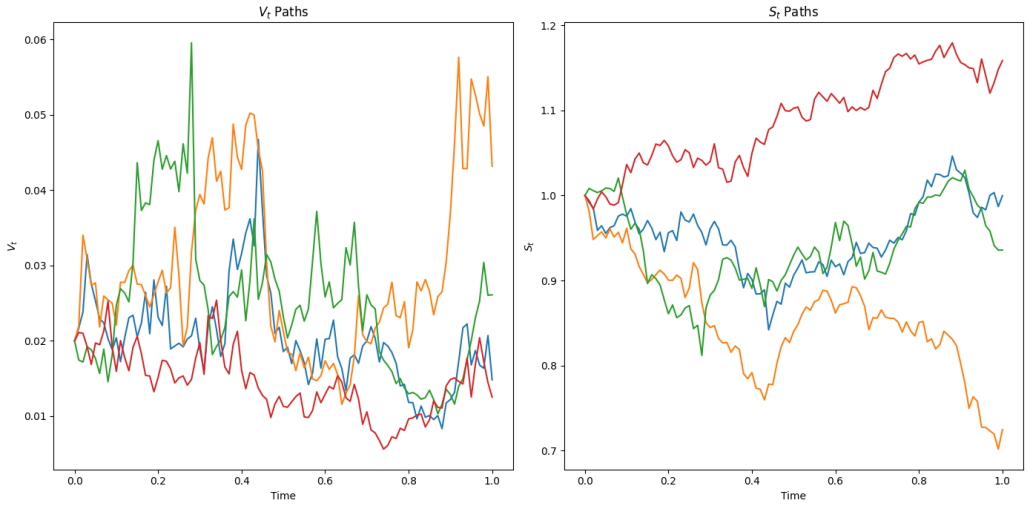

Figure 3.1: Trajectories for V_t and S_t

3. Plot the implied volatility smile in the Lifted Bergomi model for $n = 5, 10, 20$
Using $T = 1$ and nb_scenario = 10,000 with 20 equidistant log strikes between -0.3 and 0.3, we have

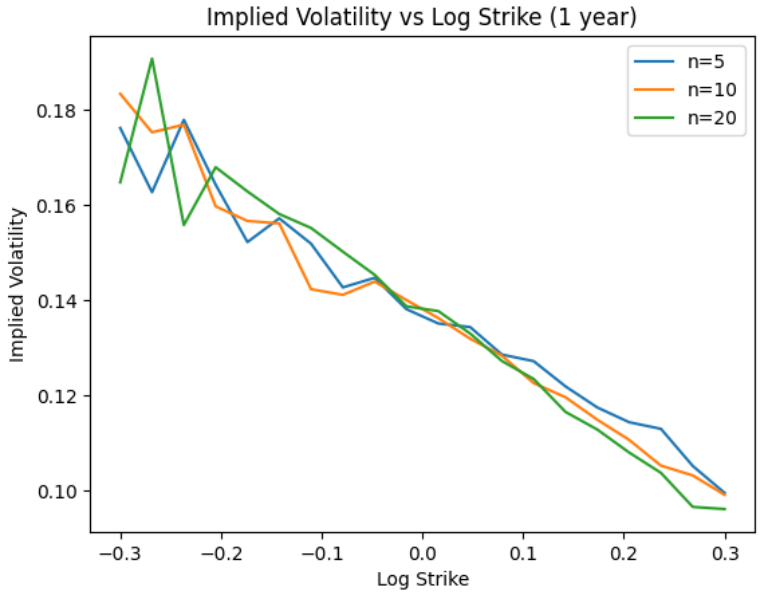

Figure 3.2: Implied Volatility vs Log Strike (1 year)

- The implied volatility behavior for ITM, ATM, and OTM are the same compared with the Lifted Heston case
- The complexity of the model might lead to the Monte Carlo simulation exhibiting more noise, which might contribute to the irregularities and spikes in the graph
- The number of factors in the model seems to affect the smoothness of the resulting implied volatility curves. Curves with a higher number of factors appear smoother, suggesting that a higher number of factors may lead to a better estimation of the implied volatilities by averaging out some of the noise inherent in the simulation process.

4. Options on VIX

For question 4.1, all the derived functions with detailed steps are shown in the Jupyter Notebook Exercise 4.ipynb

1. In this part, we specify Heston's stochastic volatility model and provide details on computing the option's prices. We use the following notations:

   - **S(t)**: Equity spot price (in our case VIX value).
   - **v(t)**: Variance.
   - **C**: European call option price.
   - **K**: Strike price.
   - $W_{1,2}$: Standard Brownian movements.
   - **r**: Interest rate.
   - κ: Mean reversion rate.
   - θ: Long run variance.
   - v_0: Initial variance.
   - σ: Volatility of variance.
   - ρ: Correlation parameter.
   - t_0: Current date.
   - T: Maturity date.

   Heston's Stochastic Volatility Model under real-world probability measure is specified as follows:

$$\begin{cases} dS(t) = \mu S(t)dt + \sqrt{v(t)}S(t)dW_1(t) \\ dv(t) = \kappa(\theta - v(t))dt + \sigma\sqrt{v(t)}dW_2(t) \\ \rho dt = dW_1(t)dW_2(t) \end{cases} \tag{4.1}$$

   Using Girsanov's Thereom to change to the risk-neutral probability $\mathcal{Q}$, we find that Heston's Stochastic Volatility Model under $\mathcal{Q}$ is given by:

$$\begin{cases} dS(t) = rS(t)dt + \sqrt{v(t)}S(t)dW_1(t)^{\mathcal{Q}} \\ dv(t) = \kappa^{\mathcal{Q}}(\theta^{\mathcal{Q}} - v(t))dt + \sigma\sqrt{v(t)}dW_2(t)^{\mathcal{Q}} \\ \rho^{\mathcal{Q}}dt = dW_1(t)^{\mathcal{Q}}dW_2(t)^{\mathcal{Q}} \end{cases} \tag{4.2}$$

   $\rho^{\mathcal{Q}} = \rho$, $\kappa^{\mathcal{Q}} = \kappa + \lambda$, $\theta^{\mathcal{Q}} = \frac{\kappa\theta}{\kappa+\lambda}$

Where: λ **is the variance risk premium**.

By applying the Ito lemma and standard arbitrage arguments, we arrive at Garman's partial differential equation:

$$\frac{\partial C}{\partial t} + \frac{S^2 v}{2}\frac{\partial^2 C}{\partial S^2} + rS\frac{\partial C}{\partial S} - rC + [\kappa(\theta - v) - \lambda v]\frac{\partial C}{\partial v} + \frac{\sigma^2 v}{2}\frac{\partial^2 C}{\partial v^2} + \rho\sigma Sv\frac{\partial^2 C}{\partial S \partial v} = 0 \quad (4.3)$$

Heston builds the solution of the partial differential equation using characteristic functions. He developed the solution in the form corresponding to the Black and Scholes model [2]:

$$C(S0, K, v0, \tau) = SP_1 - Ke^{-r\tau}P_2 \quad (4.4)$$

Where:

- P_1: Delta of the European call option.
- P_2: Conditional risk-neutral probability that the asset price will be greater than K at the maturity.

Both probabilities $P_{1,2}$ also satisfy the PDE (4.3). Provided that characteristic functions φ_1 and φ_2 are known the terms $P_{1,2}$ are defined via the inverse Fourier transformation:

$$P_j = \frac{1}{2} + \frac{1}{\pi}\int_0^\infty \Re\left(\frac{e^{-i\phi\ln(K)}\varphi_j(X_0, K, v_0, \tau; \phi)}{i\phi}\right) d\phi \quad j = 1, 2 \quad (4.5)$$

With $X = ln(S)$

Heston assumes the characteristic functions φ_1 and φ_2 having the form:

$$\varphi_j(X_0, K, v_0, \tau; \phi) = e^{C_j(\tau;\phi) + D_j(\tau;\phi) + i\phi X} \quad \tau = T - t \quad (4.6)$$

With:

$$C_j(\tau;\phi) = r\phi i\tau + \frac{a}{\sigma^2}\left[(b_j - \rho\sigma\phi i + d)\tau - 2ln\left[\frac{1 - e^{d\tau}}{1 - ge^{d\tau}}\right]\right]$$

$$D_j(\tau;\phi) = \frac{b_j - \rho\sigma\phi i + d}{\sigma^2}\left[\frac{1 - e^{d\tau}}{1 - ge^{d\tau}}\right]$$

Where:

- $g = \frac{b_j - \rho\sigma\phi i + d}{b_j - \rho\sigma\phi i - d}$
- $d = \sqrt{(\rho\sigma\phi i - b_j)^2 - \sigma^2(2u_j\phi i - \phi^2)}$
- $u_1 = 0.5$, $u_2 = -0.5$, $a = \kappa\theta$
- $b_1 = \kappa + \lambda - \rho\sigma$, $b_2 = \kappa + \lambda$

To simplify the call price formula, we write the Heston call price in the form (**that's the form that we used in the Python implementation**):

$$C(S_0, K, v_0, \tau) = \frac{1}{2}(S_0 - Ke^{-r\tau}) + \frac{1}{\pi}\int_0^\infty \Re\left(e^{r\tau}\frac{\varphi(\phi - i)}{i\phi K^{i\phi}} - K\frac{\varphi(\phi)}{i\phi K^{i\phi}}\right) d\phi \quad (4.7)$$

With:

$$\varphi(X_0, K, v_0, \tau; \phi) = e^{r\phi i\tau} S^{i\phi} \left[\frac{1 - ge^{d\tau}}{1 - g}\right]^{\frac{-2a}{\sigma^2}} \exp\left[\frac{a\tau}{\sigma^2}(b_2 - \rho\sigma\phi i + d) + \frac{v_0}{\sigma^2}(b_2 - \rho\sigma\phi i + d)\left[\frac{1 - e^{d\tau}}{1 - ge^{d\tau}}\right]\right]$$

With:

- $d = \sqrt{(\rho\sigma\phi i – b)^2 + \sigma^2(\phi i + \phi^2)}$
- $g = \frac{b - \rho\sigma\phi i + d}{b - \rho\sigma\phi i - d}$
- $a = \kappa\theta$
- $b = \kappa + \lambda$

We display below some examples of VIX options volatility smiles using different sets of parameters:

Parameters	$Example_1$	$Example_2$	$Example_3$
VIX_0	18	15	10
v_0	0.04	0.06	0.05
κ	1.5	3	4
θ	0.04	0.07	0.1
σ	0.3	0.4	0.5
ρ	-0.5	-0.8	-0.8
λ	0.5	0.3	0.3
τ	1	0.8	0.6
r	0.05	0.05	0.05

Table 4.1: Example of parameters to plot VIX options volatility smiles

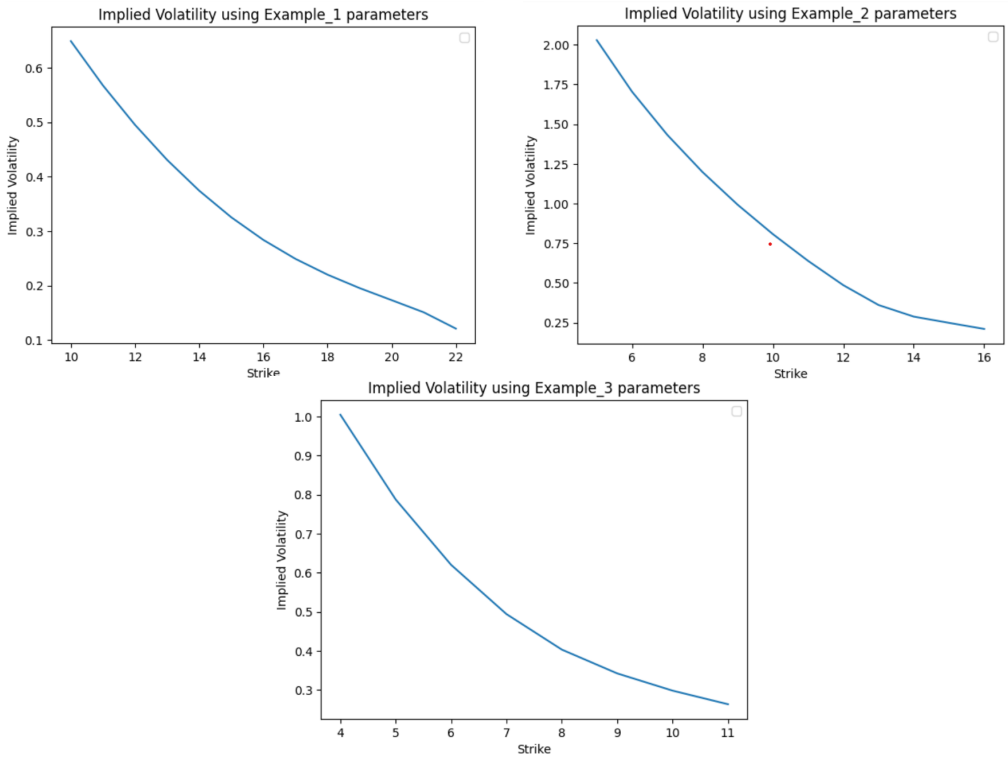

For these examples, we notice that the shape of the implied volatility is almost the same, with higher volatilities for lower strikes, which is close to the (expected) behavior of the volatility implied from the market prices using the Black-Scholes formula.

Remark: Since the model's parameters are not calibrated when the value of the strike is high (for example, for $Example_1$ parameters if strike > 24, the Heston model underprices the option, which raises the error: "BelowIntrinsicException: The volatility is below the intrinsic value." when trying to calculate the Implied volatility. The same remark occurs when the time to maturity τ is high (more than 3 years in case of $Example_1$ parameters).

Model Calibrtion (extension)

We tried to calibrate the model's parameters to overcome these issues using the available Yahoo Finance VIX options data. The details of the market data extraction and preprocessing are provided in the notebook.

The calibrated parameters are given in the table below:

Parameters	Value
v_0	1.85
κ	1.183
θ	0.242
σ	1.0
ρ	-1.0
λ	-1.836

Table 4.2: Calibrated parameters for the Heston model

These parameters suggest that:

- The variance process starts at 185%.
- $\kappa = 1.183$ implies a moderate mean reversion speed.
- $\theta = 0.242$ suggests a relatively low long-run variance.
- $\sigma = 1.0$ suggests a high volatility of the variance process.
- $\rho = -1$ suggests a strong negative correlation between the underlying process (VIX in this case) and the volatility process.
- $\lambda = -1.836$ λ accounts for the risk premium associated with volatility. A value of -1.836 suggests that investors demand compensation for bearing volatility risk.

Using these parameters, and by setting the initial value of the VIX equal to 15 and maturity equal to 6 months, we can plot the following volatility smile:

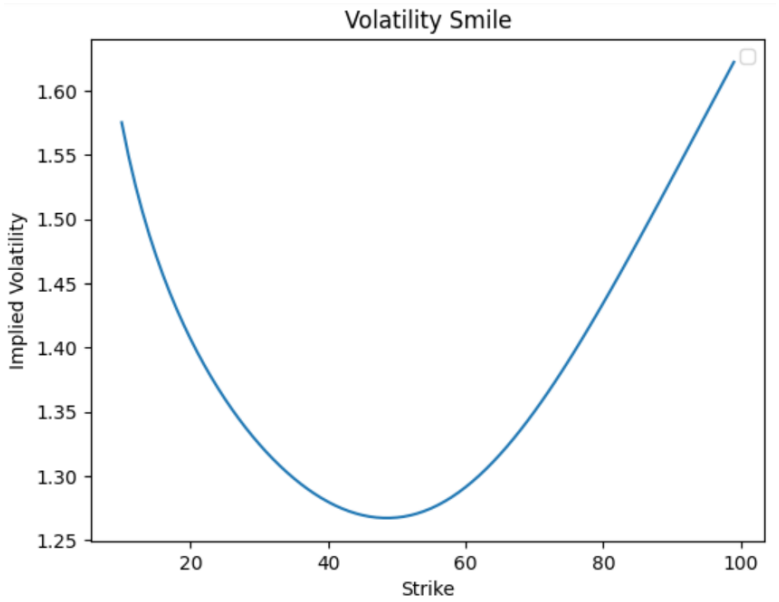

Figure 4.3: Volatility Smile using the calibrated parameters (6 months)

We observe that the volatility smile is very well pronounced, with higher implied volatilities for low and high strikes, and lower implied volatilities around the strike 50.

Comparision with the volatility smile implied by the market:

Using the calibrated parameters from table (4.2), and a maturity of 199 days (the largest maturity available in our extracted market data), we display a comparision between the volatility smile using Heston Model with calibrated parameters and the volatility smile implied by the market (The initial value of the VIX is equal to 13):

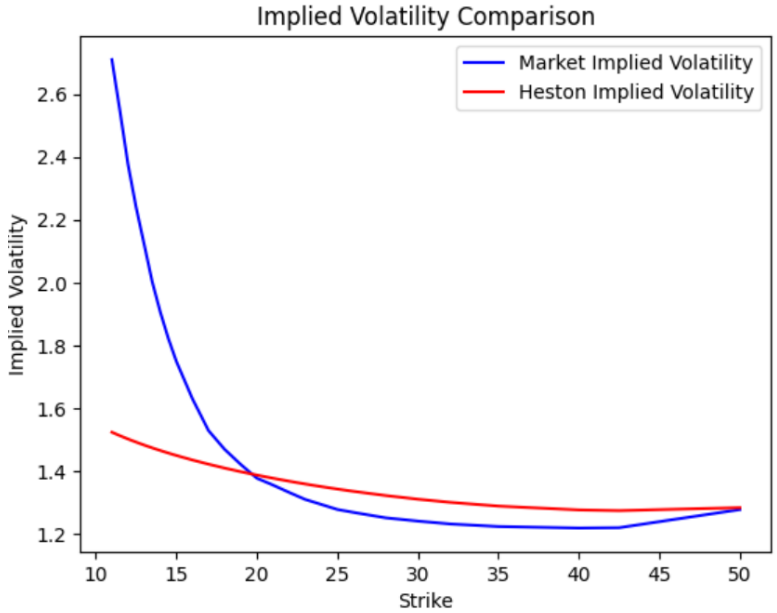

Figure 4.4: Market Implied Volatilities Vs Hestion Implied Volatilities (199 days)

We notice that the Heston model fails in reproducing the explosive behavior of the implied volatility observed in the market for low strikes. For the strike values greater than 20, we observe that calibrated Heston model is able to capture the market implied volatility with low estimation errors.

2. To price options on VIX using the Lifted Heston and Bergomi models, we first need to understand the underlying models and their characteristics. Then, we can adapt the

pricing algorithms in exercices 2 and 3 to price options on VIX.

Lifted Heston Model

It extends the traditional Heston model by incorporating multiple factors to capture more complex dynamics of the underlying asset's volatility. This introduces additional parameters (the number of factors (n)), and it uses characteristic functions to derive option prices.

Algorithm Overview:

- **Initialisation:** define the parameters of the Lifted Heston model, including the number of discretization steps (M), maturity time (T), number of factors (n), initial volatility (v_0), mean reversion rate (κ), long-run variance (θ), volatility of variance (σ), and correlation parameter (ρ).
- **Characteristic Function Implementation:** Implement the characteristic function of the Lifted Heston model, which is used to derive option prices.
- **Carr-Madan Formula:** Use the Carr-Madan formula to compute option prices based on the derived characteristic function. Which involves numerical integration over the characteristic function and applying appropriate transformations to obtain call prices.
- **Calibrate the model:** Calibrate the parameters (κ, θ, σ, ρ, v_0, λ, ...) of the model to the market VIX option prices, using techniques similar to the calibration of the standard Heston model. This ensures that the model accurately captures the observed option prices.

Lifted Bergomi Model

It is another extension of the traditional Heston model, focusing on capturing the roughness and skewness of the volatility surface. The model introduces the Hurst exponent (H) and uses stochastic integrals to model volatility dynamics.

Algorithm Overview:

- **Initialisation:** Specify the parameters of the Lifted Bergomi model, including the maturity time (T), number of discretization steps (M), Hurst exponent (H), initial VIX value (S0), initial volatility (v_0), mean reversion rate (κ), volatility of variance (σ), correlation parameter (ρ), and number of factors (n).
- **Simulation of Stochastic Processes:** Develop a method to simulate the stochastic processes involved in the Lifted Bergomi model (the evolution of volatility and the underlying asset price).
- **Option Price Calculation:** Implement a pricing method that calculates option prices based on simulated paths of the underlying asset price.
- **Calibrate the model:** Calibrate the parameters (κ, θ, σ, ρ, v_0, λ, ...) of the model to the market VIX option prices, using techniques similar to the calibration of the standard Heston and Bergomi models. This ensures that the model accurately captures the observed option prices.

Comparison with Standard Heston Model:

- **Complexity:** Both the Lifted Heston and Bergomi models offer increased complexity compared to the standard Heston model due to the incorporation of additional

parameters and factors, but from a practical viewpoint, it's demonstrated [1] that the lifted Heston model calibrates twenty times faster than its rough counterpart and is easier to simulate than the rough model.

- **Market Capturing:** The standard Heston model fails to reproduce the at-the-money skew of the implied volatility observed in the market (for short maturities), whereas the Lifted Heston model and the Rough Heston model reproduce the same volatility surface as the market for maturities ranging from one week to two years [1], and they both mimic the explosion of the at-the-money skew for short maturities.

In summary, while the standard Heston model provides a solid framework for option pricing, the Lifted Heston and Bergomi models offer enhanced capabilities for modeling complex volatility dynamics, making them potentially better suited for pricing VIX options. However, implementing algorithms for these models requires careful consideration of their unique characteristics and computational complexities.

References

[1] Eduardo Abi Jaber. Lifting the heston model. *AXA Investment Managers, Multi Asset Client Solutions, Quantitative Research. Université Paris-Dauphine, PSL University, CNRS, CEREMADE*, 2019.

[2] Sergei Mikhailov and Ulrich Nögel. Heston's stochastic volatility model implementation, calibration and some extensions. *Fraunhofer Institute for Industrial Mathematics, Kaiserslautern, Germany*, pages 74–79.